



Heriot-Watt University  
Research Gateway

## Measurements of Submicron Particle Adsorption and Particle Film Elasticity at Oil-Water Interfaces

**Citation for published version:**

Manga, MS, Hunter, TN, Cayre, OJ, York, DW, Reichert, MD, Anna, SL, Walker, LM, Williams, RA & Biggs, SR 2016, 'Measurements of Submicron Particle Adsorption and Particle Film Elasticity at Oil-Water Interfaces', *Langmuir*, vol. 32, no. 17, pp. 4125-4133. <https://doi.org/10.1021/acs.langmuir.5b04586>

**Digital Object Identifier (DOI):**

[10.1021/acs.langmuir.5b04586](https://doi.org/10.1021/acs.langmuir.5b04586)

**Link:**

[Link to publication record in Heriot-Watt Research Portal](#)

**Document Version:**

Publisher's PDF, also known as Version of record

**Published In:**

Langmuir

**General rights**

Copyright for the publications made accessible via Heriot-Watt Research Portal is retained by the author(s) and / or other copyright owners and it is a condition of accessing these publications that users recognise and abide by the legal requirements associated with these rights.

**Take down policy**

Heriot-Watt University has made every reasonable effort to ensure that the content in Heriot-Watt Research Portal complies with UK legislation. If you believe that the public display of this file breaches copyright please contact [open.access@hw.ac.uk](mailto:open.access@hw.ac.uk) providing details, and we will remove access to the work immediately and investigate your claim.

## Measurements of Submicron Particle Adsorption and Particle Film Elasticity at Oil–Water Interfaces

Mohamed S. Manga,<sup>\*,†</sup> Timothy N. Hunter,<sup>†</sup> Olivier J. Cayre,<sup>†</sup> David W. York,<sup>†</sup> Matthew D. Reichert,<sup>‡</sup> Shelly L. Anna,<sup>‡</sup> Lynn M. Walker,<sup>‡</sup> Richard A. Williams,<sup>‡,§</sup> and Simon R. Biggs<sup>†,⊥</sup>

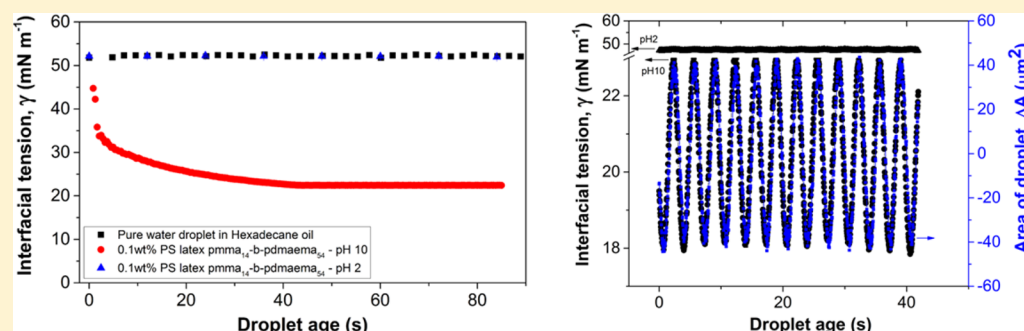
<sup>†</sup>School of Chemical and Process Engineering, University of Leeds, Woodhouse Lane, Leeds LS2 9JT, United Kingdom

<sup>‡</sup>Department of Chemical Engineering, Carnegie Mellon University, Pittsburgh, Pennsylvania 15213, United States

<sup>§</sup>Heriot-Watt University, George Heriot Wing, Edinburgh, EH14 4AS, United Kingdom

<sup>⊥</sup>School of Chemical Engineering, The University of Queensland, Brisbane, Queensland 4072, Australia

### Supporting Information



**ABSTRACT:** The influence of particle adsorption on liquid/liquid interfacial tension is not well understood, and much previous research has suggested conflicting behaviors. In this paper we investigate the surface activity and adsorption kinetics of charge stabilized and pH-responsive polymer stabilized colloids at oil/water interfaces using two tensiometry techniques: (i) pendant drop and (ii) microtensiometer. We found, using both techniques, that charge stabilized particles had little or no influence on the (dynamic) interfacial tension, although dense silica particles affected the “apparent” measured tension in the pendant drop, due to gravity driven elongation of the droplet profile. Nevertheless, this apparent change additionally allowed the study of adsorption kinetics, which was related qualitatively between particle systems by estimated diffusion coefficients. Significant and real interfacial tension responses were measured using  $\sim 53$  nm core–shell latex particles with a pH-responsive polymer stabilizer of poly(methyl methacrylate)-*b*-poly(2-(dimethylamino)ethyl methacrylate) (pMMA-*b*-pDMAEMA) diblock copolymer. At pH 2, where the polymer is strongly charged, behavior was similar to that of the bare charge-stabilized particles, showing little change in the interfacial tension. At pH 10, where the polymer is discharged and poorly soluble in water, a significant decrease in the measured interfacial tension commensurate with strong adsorption at the oil–water interface was seen, which was similar in magnitude to the surface activity of the free polymer. These results were both confirmed through droplet profile and microtensiometry experiments. Dilational elasticity measurements were also performed by oscillation of the droplet; again, changes in interfacial tension with droplet oscillation were only seen with the responsive particles at pH 10. Frequency sweeps were performed to ascertain the dilational elasticity modulus, with measured values being significantly higher than previously reported for nanoparticle and surfactant systems, and similar in magnitude to protein stabilized droplets.

## 1. INTRODUCTION

The study of colloidal particle adsorption at liquid–liquid and liquid–air interfaces is paramount to understand the characteristics of particle-stabilized foams and emulsions<sup>1,2</sup> and to optimize development of novel functionalized materials such as colloidosomes.<sup>3,4</sup> Effectively irreversible adsorption of particles leads to the extreme stability of particle-stabilized emulsions and foams.<sup>2,5–7</sup> Once adsorbed at the interface, the particle diameter and equilibrium contact angle at the interface determine the strength of adsorption. There is significant literature in this area, most of which concerns the development of Pickering emulsions and foams, and their use as precursors

for new functional materials and so forth.<sup>8–14</sup> However, while equilibrium stabilization mechanisms are relatively well understood, generally less is known about the influence of particle adsorption on the dynamic interfacial properties which are currently the subject of differing opinion.<sup>15–18</sup> For example, pendant drop tensiometry as a method to investigate dynamic interfacial tension has been extensively used for surfactant systems at liquid–liquid interfaces; however, there are few

**Received:** December 15, 2015

**Revised:** March 14, 2016

**Published:** April 1, 2016

reports on the use of this technique to study particle adsorption.

The effect of particulates on the interfacial tension is not well understood and published data can be contradictory. Indeed, some articles conclude that adsorbed particles do not modify the interfacial tension, while others show a strong decrease of the measured interfacial tension upon particle adsorption.<sup>15–21</sup> Generally, however, it has been shown that for larger submicron- or micron-sized particle systems, the particles alone (without the competing effects of surfactants or other stabilizers) do not significantly affect interfacial tensions.<sup>6</sup> In these cases, their presence is considered instead as a third phase that displaces the liquid–liquid (or liquid–gas) contact area, but does not influence the energy of the surrounding interface. For example, Vignati et al.<sup>15</sup> investigated particles comprising a fluorescent core (300 nm) with a pure silica surface shell (0.51 and 0.77  $\mu\text{m}$  thick) produced using a modified Stöber process on iso-octane/water and octanol/water systems. The adsorption of both hydrophilic and hydrophobic particles (by hexamethyldisilazane (HMS) treatment) was not seen to modify the interfacial tension at any particle concentrations studied. Hunter et al.<sup>22</sup> compared the adsorption of  $\sim 260$  nm hydrophobic silica particles with competing adsorption of surfactant at an air–water interface to determine the impact of foam stability. They found that the particles alone had no influence on the measured dynamic surface tension, although their displacement of surrounding surfactant did influence dilatational elasticity in mixed systems.

The effect of much smaller nanoparticles (sub 20 nm) on the interfacial tension is less clear. Numerous studies have shown such particles to have an effect on the measured interfacial tension. Kutuzov et al.<sup>18</sup> investigated the adsorption of 2.3, 4.6, and 6.0 nm TOPO (trioctylphosphine oxide)-stabilized-CdSe nanoparticles to a toluene–water interface. They found that the interfacial tension decreased with increasing particle size and was also concentration dependent. Levine et al.<sup>17</sup> developed a theoretical model to calculate the oil/water interfacial tension where particles were closely packed at a planar interface. On the basis of their model, these authors reported that the interfacial tension depends on particle hydrophobicity and is seen to decrease as the contact angle increases from 0° to 90°. Stocco et al.<sup>23</sup> studied 20 nm silica particles at the air/water interface. They found that the change in interfacial tension was concentration dependent. Du et al.<sup>24</sup> studied the adsorption energy of 2.5, 5, and 10 nm citrate-stabilized gold nanoparticles on octafluoropentyl acrylate (OFPA)/water interface and found that the decrease in interfacial tension was particle concentration dependent. This observation was also matched by Ferdous et al.<sup>25</sup> using alkanethiol-stabilized gold nanoparticles ( $\sim 1.7$  and 2.8 nm) at the hexane–water interface.

On the contrary, Drelich et al.<sup>16</sup> showed little or no effect on the interfacial tension from adsorption of 12 nm hydrophobic fumed silica particles at the paraffin oil/water interface. Kotula and Anna<sup>19</sup> investigated the adsorption of 12 nm Ludox silica particles stabilized with sodium aluminate onto a bubble and also found that the particles did not influence the measured interfacial tension, highlighting that even in cases of small nanoparticle adsorption, the resulting behavior is difficult to predict.

Particulate systems with amphiphilic behavior have also been studied at interfaces. In 2006, Glaser et al.<sup>26</sup> studied the interfacial activity of Janus nanoparticles (consisting of iron oxide  $\text{Fe}_3\text{O}_4$  hydrophilic particles and gold hydrophobic

particles with an overall diameter of 14 nm) at the hexane/water interface. They found that the interfacial activity could be influenced by increasing the amphiphilic character of the particles. Kim et al.<sup>20</sup> found that amphiphilic graphene oxide (consisting of a hydrophobic basal plane of polyaromatic islands of unoxidized benzene rings with hydrophilic ionizable edge-COOH groups) lowered the interfacial tension of a toluene–water interface as a function of pH. The size of the sheets used were bimodal consisting of (a) smaller pieces  $\leq 1$   $\mu\text{m}$  and (b) larger pieces  $> 5$   $\mu\text{m}$ .

It has been shown previously that the presence of a surface-active polymer on the surface of nanoparticles can make them extremely efficient emulsifiers. To date, influence of particle adsorption behavior at liquid–liquid interfaces of such systems is very limited. Isa et al.<sup>27</sup> qualitatively studied the self-assembly of iron oxide core–shell particles (where the core particle size is varied up to 5 nm and the shell is composed of poly(ethylene glycol) polymer) at the *n*-decane/water interface. They reported that the bulk concentration of particles and the molecular weight of the polymer both have a strong influence on the adsorption kinetics. The same authors also studied nanoparticles with a PEG-shell and reported a reduction in the interfacial tension related to the presence of the polymer shell on the particle surface.<sup>28</sup> Recently, Alvarez et al.<sup>29</sup> investigated the adsorption of 20 nm silica particles grafted with poly(2-(dimethylamino)ethyl methacrylate) (pDMAEMA) polymer at the air–water and xylene–water interfaces using a micro-tensiometer device. It was postulated that the reduction in the measured interfacial tension was due to the polymer on the particles penetrating the interface and relaxing to a flatter conformation to maximize the surface contact. Furthermore, the interfacial tension decreased with increasing particle concentration.

The role of particles on the interfacial tension differ markedly between specific systems as highlighted above, and are further complicated by presence/addition of surface active species such as surfactants and impurities either in the bulk or at the interface. In addition, when using dense particles the interface can deform when measuring interfacial activity due to gravitational effects, which can be wrongly interpreted. Hence, in this paper we aim to more completely probe particle type and particle concentration dependence of oil–water interfacial tension using (a) large “bare” charge stabilized colloidal particulate systems of different densities and (b) sub-100 nm particles grafted with a pH responsive and surface-active polymer, to understand the role of the stabilizer on surface activity. Pendant drop tensiometry and microtensiometry are used as two comparative techniques operating at two different length scales and allows the decoupling of gravitational settling effects of the particles. In addition, the micro-tensiometer is used to investigate the interfacial rheology by oscillation of the interface to determine the dilatational modulus with the different particles.

## 2. EXPERIMENTAL SECTION

**2.1. Materials.** The silica used here was purchased from FUSO Chemical Co. Ltd., Japan. The particle size was nominally 800 nm, as confirmed by light scattering (Malvern Zetasizer ZS) with low polydispersity, (PDI  $\sim 0.1$ ). 300 nm sulfate stabilized polystyrene latex particle were purchased from the Interfacial Dynamics Corporation (IDC), U.S.A. Polystyrene latex particles grafted with poly(methyl methacrylate)-*b*-poly(2-(dimethylamino)ethyl methacrylate) (pMMA-*b*-pDMAEMA) were also used in this study. The average particle size based on SEM micrographs was  $53 \pm 3$  nm. Details regarding their

synthesis are provided in section 2.2.1. To remove impurities tricaprylin (purity  $\geq 99\%$ , Sigma-Aldrich), *n*-hexadecane (purity  $\geq 99\%$ , Sigma-Aldrich) were passed through an alumina column 5 times.

## 2.2. Methods. 2.2.1. Synthesis of the Responsive Latex Particles.

The polystyrene latex particles were prepared via an emulsion polymerization in a batch mode at 70 °C, using previously reported protocols.<sup>12,30,31</sup> For more details see Supporting Information S1.

**2.2.2. Particle Characterization of Responsive Late Particles.** The hydrodynamic diameter of these particles across a range of pH from 2.5 to 10.5 was measured using dynamic light scattering (Malvern Zetasizer, Malvern Instruments, U.K.). The same instrument was used to determine the electrophoretic mobility of the particles across the same pH range. The pH of the particle dispersion was changed using 0.1 M HNO<sub>3</sub> and KOH solutions with a background electrolyte concentration of 10 mM KNO<sub>3</sub>. Scanning electron microscopy (SEM) images were obtained from a LEO 1530 Field Emission Gun SEM operating at 3 kV.

**2.2.3. Interfacial Tension Using Pendant Drop Tensiometry.** The dynamic interfacial tension was measured using a series of colloidal dispersions of varying concentrations. The measurements were carried out using a drop shape analysis system (DSA100, Krüss, Germany). The equipment was calibrated by measuring the pure air–water surface tension until a value of 72.8 mN m<sup>-1</sup> was obtained. Single droplets (50  $\mu$ L unless specified) of the dispersion were formed at the end of a steel needle (1.84 mm) (at a flow rate of 200  $\mu$ L min<sup>-1</sup>) placed in the oil phase within a cuvette and images were recorded using a CCD camera over a period of time at 20 °C. Each measurement was started (in all experiments) as soon as the droplets were expressed from the syringe ( $t_0 = 0$ ). The profile of the droplet in each image was detected automatically using the analysis software package DSA3 (Krüss, Germany) and fitted to the Young–Laplace equation to obtain interfacial tension values as a function of time. The pure interfacial tensions of (a) a tricaprylin oil/water (pH 6, 0.1 M NaCl) interface and (b) a hexadecane oil/water (pH 2, 0.1 M KNO<sub>3</sub>) were measured and calibrated based on values reported in the literature.<sup>32,33</sup> The effect of (1) silica on a tricaprylin/water interface, (2) polystyrene sulfate latex and (3) pH-responsive latex particles on a hexadecane/water interface were then measured. These particle and oil pairings were chosen as preliminary bulk emulsion studies (Figure S4 in Supporting Information), and previous studies in the literature<sup>12,30,34–36</sup> have demonstrated that the particles have high affinity for the oil–water interfaces and do produce stable emulsions. A summary of these pairings is presented in Table 1.

**Table 1. Summary of Particle and Oil Pairings Used in This Study and at Similar Interfaces in the Literature**

	1	2	3
Particle	800 nm FUSO Silica	300 nm sulfate stabilized polystyrene latex	53 nm pMMA- <i>b</i> -pDMAEMA stabilized polystyrene latex particles
Particle Density (kg/m <sup>3</sup> )	2200	1050	1050
Oil phase	Tricaprylin	<i>n</i> -Hexadecane	<i>n</i> -Hexadecane
References	34	35	30

**2.2.4. Interfacial Tension Using Microtensiometer.** Interfacial tension measurements were also performed using a microtensiometer device, described elsewhere.<sup>37,38</sup> In summary, the device contains a pressure transducer which is in-line with a capillary filled with the oil phase. The capillary is immersed in a 3.5 mL well containing the particle dispersion. The bottom wall of the device has a 30 mm circular glass slide. The glass capillaries are produced in the same manner as reported previously,<sup>38</sup> with a tip radius of 40  $\mu$ m (unless otherwise noted). In a typical experiment, the glass capillaries were cleaned using sulfuric acid and rinsed with acetone. The capillaries were washed with acetone for a number of times and allowed to dry in an oven. Once dried, the capillaries were tested for axis-symmetry using a microscope

and to ensure that the tip of the capillary was not damaged by the cleaning procedure.

The equipment was calibrated by measuring the pure air–water surface tension until a value of 72.8 mN m<sup>-1</sup> was obtained after which the pure liquid–liquid interfacial tension was measured. The pure interfacial tensions of (a) a tricaprylin oil/water interface and (b) a hexadecane oil/water were measured and calibrated based on values reported in the literature.<sup>32,33</sup> The cell was cleaned and replaced with a particle dispersion to be studied. An oil droplet with a radius of  $R_d = 40 \mu$ m was formed using a constant pressure head (generated by a water column connected to the 3-way solenoid valve). The interface was recorded using a Diagnostic Instrument Spot RT Monochrome digital camera connected to the microscope. LabVIEW was used to process recordings of the interface to determine changes in the droplet radius and to monitor the pressure changes (subtraction of the hydrostatic pressure head at the capillary tip from the measured constant pressure head) to attain interfacial tension measurements. It should be noted that measurement of the tricaprylin–water interfacial tension was started as soon as the droplets were expressed from the syringe in the device ( $t_0 = 0$ ).

**2.2.5. Dilational Modulus Measurements Using Microtensiometer.** Dilational elasticity measurements were performed by oscillating the 40  $\mu$ m droplet, once the equilibrium interfacial tension had been obtained for the sterically stabilized latex particles. This was done by changing the constant pressure head to the oscillatory pressure head, which can be varied over a frequency range of 0.15–2 Hz at an amplitude of about 50–100 Pa. The corresponding changes in the interfacial tension with this drive signal were measured. The dilational elasticity modulus<sup>39</sup> is calculated by measuring the change in stress due to change in interfacial area of an interface.

In the case where we investigate multiple frequencies for the same adsorbed particle monolayer, after oscillating the interface at a specific frequency, the interface is allowed to relax for  $\sim 500$  s before oscillating at a new frequency.

## 3. RESULTS AND DISCUSSION

**3.1. Nonresponsive Systems. 3.1.1. Pendant Drop Tensiometry.** To allow for comparison with the behavior of the pH-responsive polymer stabilized particles, the apparent interfacial tension of the “bare” charge stabilized silica and sulfate-stabilized polystyrene latex samples were initially measured at the tricaprylin–water and hexadecane–water interfaces, with varying particle concentration from 0.1 to 4 wt %, as shown in Figure 1.

The silica data in Figure 1a indicate a change in the “apparent” interfacial tension as a function of particle concentration: These values are calculated automatically by the instrument software from observed deformations of the interface. While for a two-dimensional interface, these deformations are assumed to result solely from changes to the oil–water surface tension, when particles are present this may no longer be the case. The analysis of the adsorption process in the pendant drop when using relatively large silica particles is complicated by gravitational settling.<sup>23</sup> Due to density differences the silica particles will sediment over time, and this can lead to particles collecting at the base of the droplet. This sedimentation will cause a deformation in the droplet shape due to the weight of particles collecting at the bottom of the drop (illustrated by the dashed line in Figure S2.1a in the Supporting Information); which will influence the drop shape and therefore create an apparent change in the interfacial tension measurement when compared to a pure water droplet (Figure S2.1b in Supporting Information). Performing Stokes’ settling calculations (assuming no hindered settling) indicates that the particles will settle at a velocity of  $10^{-10}$  m/s meaning that the time taken for a particle to settle



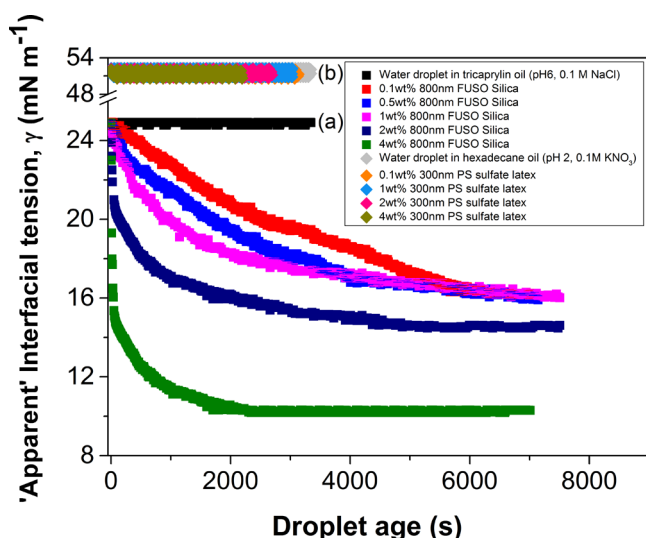


**Figure 1.** Dynamic “apparent” interfacial tension of (a) a water droplet (pH 6, 0.1 M NaCl) containing 800 nm silica colloids dispersed at various particle concentrations immersed in tricapylin oil at 20 °C and (b) a water droplet (pH 2, 0.1 M  $\text{KNO}_3$ ) containing 300 nm sulfate stabilized latex particles immersed in hexadecane oil.

from the top of the droplet to the bottom will occur over  $\sim 10^3$  seconds. Experimental bulk settling times also occur in the same order of magnitude as in these experiments (Figure S2.2).

At low particle concentrations of 0.1 to 1 wt %, all isotherms reach an equilibrium “apparent” interfacial tension value of 16.1  $\text{mN m}^{-1}$ . The fact that all values are almost identical indicates that similar particle coverage (likely a monolayer) is perhaps achieved in each case and suggests that any buildup of deposits at the base of the drop is negligible. At these concentrations change in the droplet shape will be driven by the added weight of the adsorbed monolayer. The time taken to reach the equilibrium value clearly decreases with increasing particle concentration.

As the particle concentration is increased above 1 wt % the isotherms show an initial rapid drop in interfacial tension after which it slows and reaches an equilibrium tension value of 15.4 and 10.3  $\text{mN m}^{-1}$  at 2 and 4 wt %, respectively (much faster in comparison to concentrations  $\leq 1$  wt %). The drastic change in the isotherms at these higher concentrations is more likely to be driven by the added weight of the particle bed forming at the bottom of the droplet rather than any “real” dynamic interfacial tension change. However, we note here that these silica particles are expected to adsorb to the oil–water interface as they have been shown to efficiently stabilize tricapylin in water emulsions at pH 6 and in the presence of 0.1 M NaCl.<sup>34,36</sup> Additionally, while such “apparent” changes may not indicate true interfacial tension effects, these measurements may be useful to study adsorption kinetics for the silica. It should also be noted that studies with smaller unmodified silica have also shown no influence on the measured dynamic surface tension.<sup>22,40</sup>

In order to eliminate sedimentation effects, the adsorption of 300 nm sulfate stabilized polystyrene latex “model” particles at the hexadecane/water interface was also investigated, since the density of polystyrene (1.05  $\text{g cm}^{-3}$ ) is much closer to that of water. It should be noted that the latex particles were cleaned thoroughly via numerous centrifugation and redispersion cycles (typically 8–10 cycles), until the supernatant matched the air/

water surface tension value  $72.8 \pm 0.2$   $\text{mN/m}$ . This is to ensure that no impurities remain in the particle dispersion that could influence the measured dynamic interfacial tension. Once cleaned, the particles were retested at the hexadecane/water interface to measure the dynamic interfacial tension at 20 °C (Figure 1b).

It is clear from Figure 1b that the addition of the clean particles led to no measured effect on the interfacial tension. The lower density of latex (close to mutual buoyancy in water) obviously causes very little distortion based on the gravitational weight of the interface when compared with the silica sample (Figures 1a and S2.1). Since both the silica particles and the latex particles have been shown to adsorb at the oil/water interface, as inferred from the stabilization of emulsions,<sup>7,29</sup> it is concluded that their adsorption does not alter the true interfacial tension.

**3.1.2. Microtensiometry.** It should be noted that in the microtensiometer, the interfacial tension of an oil droplet in water is measured, rather than a water droplet in oil, as was used for the pendant drop experiments. Also, the particle concentrations used in the microtensiometer were much lower than that used in the pendant drop device. This is because at higher particle concentrations it is difficult to image the interface due to the opaqueness of the particle dispersion. Dynamic interfacial tension data for both systems are presented in Figure 2.

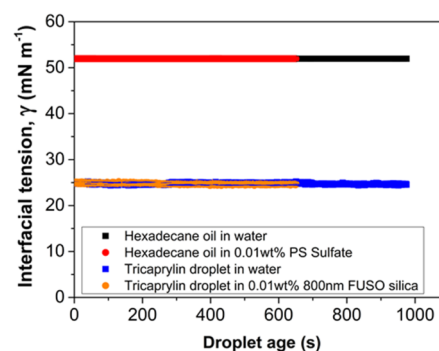


**Figure 2.** Dynamic interfacial tension of (a) a hexadecane droplet ( $R_d = 40$   $\mu\text{m}$ ) in pH 2, 0.1 M  $\text{KNO}_3$  water containing a dispersion of 0.01 wt % 300 nm sulfate-stabilized silica polystyrene latex particles; and (b) a tricapylin droplet ( $R_d = 40$   $\mu\text{m}$ ) in pH 6, 0.1 M NaCl water containing a dispersion of 0.01 wt % 800 nm silica colloids..

The addition of 0.01 wt % 800 nm FUSO silica and 0.01 wt % 300 nm polystyrene sulfate latex has little/no effect on the dynamic interfacial tension and the data is effectively the same as that of a bare tricapylin/water interface and hexadecane/water interface, respectively. This observation matches data presented by Vignati et al.<sup>15</sup> and Drelich et al.,<sup>16</sup> showing that even if the bare particles are strongly attached to the interface, no reduction of interfacial tension is detected. This observation is due to the low Bond number in the microtensiometer device, which means that the droplet shape is less perturbed, i.e., the effect of gravitational forces is much reduced. Since isotherms from two techniques are the same, the data again suggests that adsorption of silica and unmodified (bare) latex particles do not change the interfacial tension.

**3.2. Responsive Systems. 3.2.1. Pendant Drop Tensiometry.** The dynamic interfacial tension of a hexadecane oil/water interface was studied using polystyrene latex particles sterically stabilized by  $\text{pMMA}_{14}\text{-}b\text{-pDMAEMA}_{54}$  (characterization of

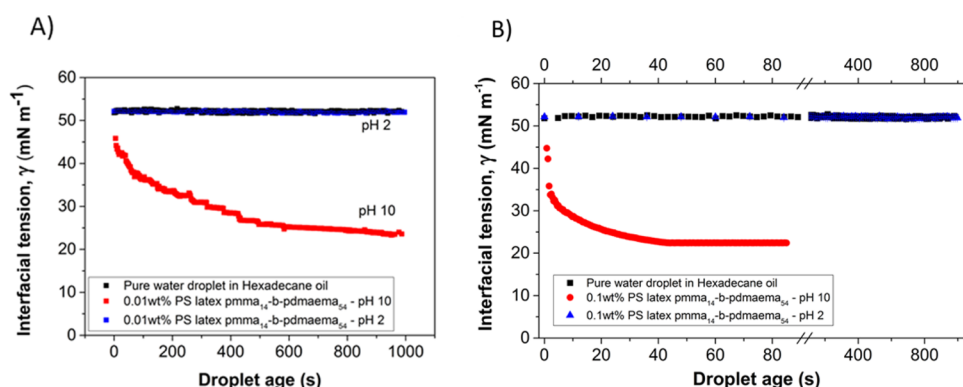


**Figure 3.** Dynamic interfacial tension of a water droplet containing (a) 0.01 wt % and (b) 0.1 wt % pMMA<sub>14</sub>-*b*-pDMAEMA<sub>54</sub> sterically stabilized polystyrene latex dispersed at pH 10 (red) and pH 2 (blue) in hexadecane oil at 20 °C.

these particles are presented in the [Supporting Information](#) section in Figures S2 and S3). During the particle synthesis, this diblock copolymer is used as the stabilizer, which anchors into the particle core via the pMMA block while the pDMAEMA block acts as a steric layer protruding from the particle surface. These particles were cleaned via dialysis, periodically changing the outer phase until the outer phase produced a surface tension value of a pure air–water interface, i.e., 72.8 mN m<sup>−1</sup>.

To investigate the effect of pH and particle concentration on the dynamic interfacial tension, the particles were prepared at pH 2 (protonated) and pH 10 (deprotonated). [Figure 3](#) illustrates the dynamic interfacial tension measured when the particles are dispersed at pH 10 and 2, respectively, at a particle concentration of 0.01 ([Figure 3a](#)) and 0.1 wt % ([Figure 3b](#)).

The interfacial tension for the bare hexadecane oil/water interface was measured to be constant at 52 mN m<sup>−1</sup>. When the interfacial tension is measured with a particle concentration of 0.01 wt % dispersed at pH 2 ([Figure 3a](#)), the dynamic interfacial tension remains unaltered, matching observations seen by Amalvy et al.<sup>30</sup> at an air–water interface. This suggests that either (a) the particles do not adsorb at the oil/water interface or (b) they do adsorb but do not affect the interfacial tension as the polymer when protonated has little affinity for the oil phase. The second mechanism is most likely here, since stabilization of oil-in-water emulsions by these particles at pH 2 has been previously demonstrated.<sup>12,31</sup>

At pH 10, the dynamic interfacial tension at  $t_0$  is lower than that observed for a bare hexadecane/water interface and for particles at pH 2. This suggests that as the droplet is produced, some particles are already adsorbed onto the liquid–liquid interface. At pH 10 the deprotonated polymer is collapsed onto the surface of the latex particle increasing its affinity for the interface and thus its adsorption. The reduction in the interfacial tension is very rapid in the first 400 s before it decreases over the next 600 s. The equilibrium interfacial tension occurs at  $\sim 23$  mN m<sup>−1</sup>. The eventual plateau in the data suggests a full coverage of the interface with core–shell latex particles with no further adsorption of surface active species.

For the particles dispersed at pH 2 (blue), increasing the particle concentration to 0.1 wt % ([Figure 3b](#)) has no or very little effect on the dynamic interfacial tension. At pH 10 (red), the interfacial tension again initially drops very rapidly before reaching an equilibrium value after approximately 40 s. The equilibrium value of the interfacial tension is 22.4 mN m<sup>−1</sup> and is similar to that seen above for the 0.01 wt % example

suggesting that, in both cases, equilibrium coverage of the interface has been achieved. The increased rate of adsorption at the higher concentration is, of course, as expected due to the higher collision rate.

Importantly, the expected adsorption kinetics of the silica and pH responsive latex can be correlated to the measured trends, by comparing the calculated Stokes–Einstein particle diffusion coefficients (across the anticipated width of the electric double layer on the surface of the droplets), of  $5.36 \times 10^{-13}$  m<sup>2</sup> s<sup>−1</sup> for the silica and  $1.01 \times 10^{-11}$  m<sup>2</sup> s<sup>−1</sup> for the latex, respectively. Due to their much smaller size, the coefficient for the latex particles is around 2.5 orders of magnitude larger, suggesting they are able to diffuse from the bulk to the interface much quicker. In addition, the number of particles in the latex system is much higher and this will lead to a high collision frequency before subsequent adsorption, although the total number of successful collisions must also increase by the same proportion for a similar complete monolayer coverage. These two competing factors make it difficult to quantitatively assess the relative interfacial affinity of the silica in respects to the latex. However qualitatively, the increased diffusion correlates closely with a much faster equilibrium interfacial tension being reached for the responsive latex particles (40 s) compared to almost 6000 s for the silica (see [Figure 1](#)) at similar particle concentrations (0.1 wt %).

To deduce whether the reduction of interfacial tension was due to primarily the polymer alone or to the composite particle–polymer system, pendant drop tensiometry data were acquired at an air–water interface for the free polymer and were compared with data obtained for charge-stabilized polystyrene latex particles and the pH responsive particles, as presented in [Figure 4](#). It is clear from these data that the charge-stabilized latex particles have no effect on the surface tension at all pH values (matching earlier observations at the oil–water interfaces presented in [section 3.1](#)). However, when investigating the free pMMA-*b*-pDMAEMA copolymer, the effect on surface tension is shown to be strongly pH dependent. At high pH, the pDMAEMA block is deprotonated (i.e. charge neutral) and the polymer display surface active properties (surface tension is around 42 mN m<sup>−1</sup> at pH 9.5). As the pH is reduced the surface activity also decreases; the pDMAEMA block becomes protonated and highly cationic, which appears to be drastically reducing the adsorption of the polymer at the interface as demonstrated by the surface tension measurements (72 mN m<sup>−1</sup>). This trend was also observed by Matsuoka et al.<sup>41</sup> using the diblock copolymer, poly(styrene)-*b*-poly(acrylic

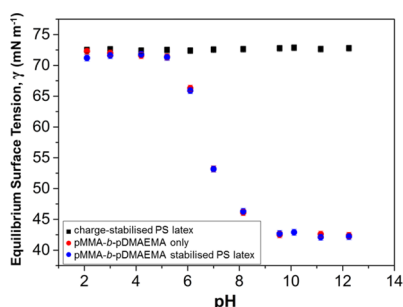


**Figure 4.** Effect of pMMA-*b*-pDMAEMA diblock copolymer and latex particles grafted with pMMA-*b*-pDMAEMA on the equilibrium air–water surface tension as a function of pH.

acid) (PSt-*b*-PAA). They reported that at pH 3 and below the AA block is protonated and behaves as a nonionic amphiphilic diblock copolymer and hence was surface active. As the pH increased to pH 10 there was no effect on the surface tension even though a cmc was observed using SLS, which corresponds to the behavior of nonsurface active polymers.

The air–water tensiometry data of the sterically stabilized latex particles presented in Figure 4 indicates almost identical pH dependent surface activity to the free polymer, which correlates to previous experimental surface tension measurements conducted at an air/water interface of similar core–shell latex systems.<sup>30</sup> Importantly, these data infer that surface activity of the core–shell particle is indeed due to the grafted polymeric stabilizer, and that such activity can be maintained from the free polymer system, allowing predictions of composite particle behavior from the polymer alone.

It can be concluded from the pendant drop tensiometry data that the adsorption of “bare” particles has little influence on the dynamic interfacial tension, where the observed reduction with high density silica particles was assumed to be due to physical droplet deformation as a result of large sedimented particle bed resting above the interface. In contrast, latex particles with a steric layer of pDMAEMA on their surface caused a significant decrease in the observed interfacial tension. In order to confirm these pendant drop tensiometry data, a study was conducted using the responsive latex particles with a microtensiometry device.

**3.2.2. Microtensiometry.** The dynamic interfacial tension of a hexadecane droplet in water was also measured in the presence of the sterically stabilized latex particles. The isotherm of the dynamic interfacial tension when the particle is dispersed at pH 2 and pH 10 is illustrated in Figure 5.

The data in Figure 5 shows that the dynamic interfacial tension of the pure interface and the latex particle-loaded interface at pH 2 are the same. At pH 2, the amine groups on the polymer are fully protonated and the resultant cationic steric layer is highly solvated by the aqueous phase and thus has little affinity for the interface. Under these conditions, the polymer is not surface active and little or no change is observed when measuring the dynamic interfacial tension despite the presence of adsorbed particles. This again matches the observation seen with the pendant drop measurements as well as with emulsion studies presented elsewhere.<sup>12</sup>

The dynamic interfacial tension when the particles are dispersed at pH 10 is also presented in Figure 5. The addition of 0.01 wt % of the sterically stabilized latex particles dispersed at pH 10 causes a significant decrease in the observed interfacial tension. Over the first 600 s as the particles adsorb, the

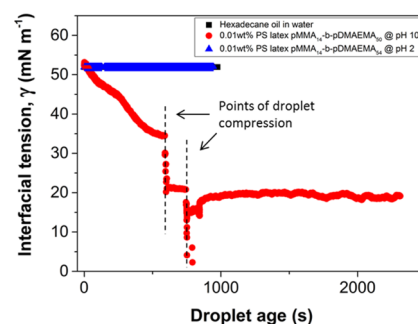


**Figure 5.** Dynamic interfacial tension of a hexadecane droplet ( $R_d = 40 \mu\text{m}$ ) in water containing a dispersion of the sterically stabilized polystyrene latex colloids dispersed at pH 2 and pH 10 at a particle concentration of 0.01 wt %. The dashed lines show two points at which there was a rapid change in the droplet size, i.e.,  $>R_d = 40 \mu\text{m}$  and thus the measured interfacial tension. At these points the droplet size had to be compressed back to  $R_d = 40 \mu\text{m}$  to continue the experiment.

interaction of the surface-active polymer at the interface causes a rapid decrease in the interfacial tension from around  $52 \text{ mN} \cdot \text{m}^{-1}$  to  $37 \text{ mN} \cdot \text{m}^{-1}$ . At around 600 s the measured interfacial tension value decreases suddenly from  $37 \text{ mN} \cdot \text{m}^{-1}$  to  $25 \text{ mN} \cdot \text{m}^{-1}$ ; interestingly, at this point the droplet size had increased sufficiently ( $>40 \mu\text{m}$ ) that it was on the verge of detachment from the capillary tip. To continue the measurement, the droplet was compressed and this sudden compression of the droplet compressed the particle monolayer at the interface, thus causing the observed large drop in interfacial tension. The interfacial tension stabilizes for about 150 s before the droplet again increases in size nearing detachment; once again the droplet is compressed and the tension value relaxes to an equilibrium value of  $19 \pm 0.5 \text{ mN} \cdot \text{m}^{-1}$ . Although the kinetics of adsorption cannot be simply deduced, due to the necessity of droplet compression, it can be postulated that adsorption kinetics are consistent with rates evidenced in the pendant drop (if one considers the much higher surface area generated in the microtensiometer).

**3.2.3. Dilational Elasticity.** Dilational elasticity measurements were performed by oscillating the  $40 \mu\text{m}$  droplet, once the equilibrium interfacial tension had been obtained for the sterically stabilized latex particles. This was done by changing the constant pressure head to the oscillatory pressure head, which can be varied over a frequency range of 0.15–2 Hz at an amplitude of about 50–100 Pa. The corresponding changes in the interfacial tension with this drive signal were measured. After oscillating the interface, the interface is allowed to relax for  $\sim 500$  s before oscillating at a new frequency.

The change in interfacial tension with changing interfacial area for the hexadecane–water interface in the presence of 0.01 wt % sterically stabilized latex particles dispersed at pH 2 and pH 10 is presented in Figure 6. Data is shown for a low oscillation (0.3 Hz) and a high oscillation (1.5 Hz) frequency.

By oscillating the interfacial area after equilibrium interfacial tension is obtained, the interface expands and contracts. During the expansion of the droplet, the interfacial area increases allowing additional particles to adsorb on the free interfacial area from bulk, while as the droplet contracts the particles on the interface rearrange and come into close contact. This oscillatory movement gives insight into the elasticity of the interface, i.e., the dilational elasticity modulus. The data in Figure 6 shows no change in the interfacial tension of particles



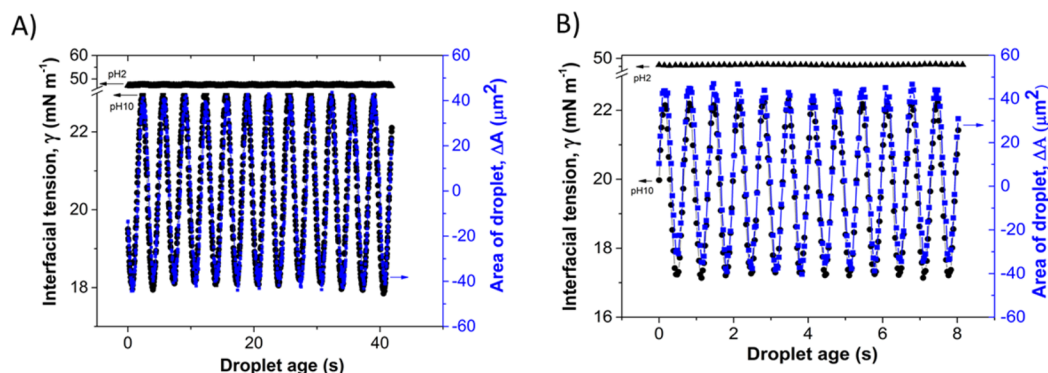


**Figure 6.** Typical plot of change in interfacial tension with changing interfacial area (squares) at an oscillation frequency of (a) 0.3 Hz and (b) 1.5 Hz of a 40  $\mu\text{m}$  hexadecane droplet in water interface laden with 0.01 wt % of sterically stabilized polystyrene latex particles dispersed at both pH 2 (triangle) and pH 10 (circle). Experiment run at 20  $^{\circ}\text{C}$ .

dispersed at pH 2 as the droplet area expands and contracts. This behavior was also seen at all frequencies tested and therefore the dilational elasticity modulus could not be calculated. This trend was also found when performing dilational elasticity measurements using both the silica and the sulfate-stabilized latex particles. This trend of low/no elasticity of pure particle layers has been previously reported by Hunter et al.<sup>22</sup> In this case, colloidal particles at an air-water interface were found to influence the interaction of co-adsorbed surfactant, but did not themselves lead to any elastic enhancement.

When the particles are dispersed at pH 10, the change in interfacial tension due to changing interfacial area is much larger. As the droplet compresses the particles come into closer contact, which causes the polymer chains that are deprotonated to entangle with each other. As the droplet expands the entangled polymer chains on the particle surface are forced to stretch giving the interface an enhanced elastic behavior. At pH 2, the polymer chains are highly protonated and are not expected to become entangled due to electrostatic repulsive interactions between the chains, and hence, the elastic properties of the particle film recorded during droplet oscillation is negligible.

By performing a frequency sweep, the dilational elasticity modulus at all frequencies can be calculated and is presented in Figure 7.

The data shows that initially, with increasing droplet oscillation frequency, the dilational elasticity modulus increases.

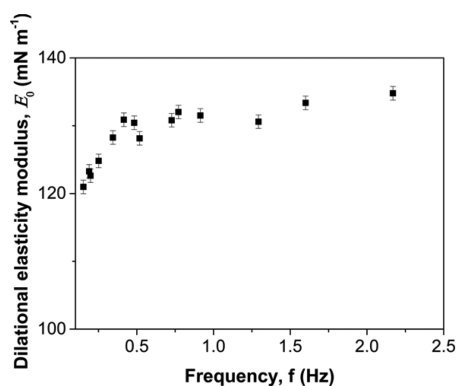


**Figure 7.** Dilational elasticity modulus of the hexadecane/water interface laden with 0.01 wt % of sterically stabilized polystyrene latex particles dispersed at pH 10, as a function of oscillation frequency.

These elasticity modulus values are much higher in comparison to adsorption of proteins, polymers, and ionic surfactants on similar interfaces.<sup>42–47</sup> As the system reaches its high frequency limit, the elasticity modulus plateaus. We suggest that this effect may be caused by two possible mechanisms.

The first is related to the adsorption rate of particles at the interface. At low droplet oscillation frequencies, the diffusion of particles from the bulk to the interface when compared to the time taken for the droplet to oscillate is proportionately faster. The particles collide with the interface and some of these collision events result in successful adsorption. As the frequency increases, the relative rate of diffusion of the particles comparing to the droplet oscillation time is reduced and hence little or no additional adsorption can occur during an oscillation event. If additional particles did adsorb during the oscillation of the interfacial area, one would expect that the interfacial tension would slowly decrease with time. This was not observed in the experiments performed. It is possible that the duration of the oscillation of experiments performed at each frequency were too small for this specific feature to be observed. Additional experiments are required here to explore this direction in more details.

The second possible mechanism relates to the interactions between polymer chains on the particles adsorbed at the interface. At low oscillation frequencies polymer layers on adjacent particles may undergo compression and stretching as the interfacial area is altered. The relaxation of polymer conformations is relatively slow and hence we would expect to see a frequency dependent effect. As the frequency increases the time for the polymer layers to adjust is reduced. This, in turn, gives less time for the chains to reorganize and may dampen the elasticity resulting in the plateau observed in the elasticity modulus data. In an earlier publication the behavior of similar particles at an air–water interface using a Langmuir trough with similar particles were described.<sup>31</sup> It was shown in this study that at pH 10, upon compression of the particle monolayer at the air–water interface, the particles aggregated and did not fully disperse upon expansion. This clearly showed a dominant adhesive feature caused by the collapsed polymer chains interacting (entangling) leading to the formation of particle aggregates. This second mechanism is thought to be a more likely explanation for the observed behavior; however, more detailed experiments are needed to gain better insights into this behavior.



## 4. CONCLUSIONS

Dynamic interfacial tension measurements show different behaviors depending on the particle system used. In the case of 800 nm FUSO silica a reduction in apparent interfacial tension was observed with increasing particle concentration, although this was thought to occur through droplet distortion on the basis of the presence of dense sedimented particle bed within the droplet being analyzed. Sulfate stabilized latex particles (of a similar density to water) were also used to investigate the dynamic interfacial tension, where it was found that for particle suspensions that were sufficiently cleaned, no visible change in the interfacial tension was obtained. Data obtained from using a microtensiometer device similarly suggested that neither system significantly reduced oil–water interfacial tension.

Results using the sterically stabilized pH responsive latex particles did however show significant surface activity. While the interfacial tension remained unaffected at pH 2, where the steric layer present on the particle surface is protonated and well solvated by the aqueous phase, at pH 10, where the polymer becomes uncharged and becomes surface active, large reductions in interfacial tension were measured using both pendant drop and microtensiometry techniques. Additionally, these changes appeared to correlate to similar activity measured at the air–water interface of the free polymer alone. Further, elasticity measurements suggested that at pH 10 the interface is extremely elastic (with modulus similar to protein type systems) as the polymer chains interlink under compression and extension as the interface is oscillated. Such behavior would suggest very strong stability of emulsion or foam systems with these surface active, and elastic, core–shell particles as interfacial stabilizers.

## ■ ASSOCIATED CONTENT

### Supporting Information

The Supporting Information is available free of charge on the ACS Publications website at DOI: [10.1021/acs.langmuir.5b04586](https://doi.org/10.1021/acs.langmuir.5b04586).

S1. Protocol for the synthesis of the responsive latex particles via emulsion polymerization. S2. Young–Laplace fits to a water droplet containing 4 wt % 800 nm silica colloids as a function of time showing droplet shape change that results in a reduction of measured interfacial tension and bulk settling test. S3a and S3b characterization data of the pH-responsive latex particles sterically stabilized with pMMA<sub>14</sub>-b-pDMAEMA<sub>54</sub>. S4. Preliminary emulsion studies showing compatibility between particle and oils chosen. (PDF)

## ■ AUTHOR INFORMATION

### Corresponding Author

\*E-mail: [M.S.Manga@leeds.ac.uk](mailto:M.S.Manga@leeds.ac.uk).

### Author Contributions

The manuscript was written through contributions of all authors. All authors have given approval to the final version of the manuscript.

### Notes

The authors declare no competing financial interest.

## ■ ACKNOWLEDGMENTS

The authors thank Dr. G. Bacquey, Dr. M. Manguian, and Dr. N. Chagneux for their help with the synthesis and characterization of the pH-responsive polymer used in this study. In addition, the EPSRC (grant number EP/G501521/1) and University of Leeds are thanked for a Ph.D. studentship and to P & G (Newcastle, U.K.) for CASE support.

## ■ REFERENCES

- (1) Binks, B. P.; Horozov, T. S. Aqueous foams stabilized solely by silica nanoparticles. *Angew. Chem., Int. Ed.* **2005**, *44* (24), 3722–3725.
- (2) Binks, B. P. Particles as surfactants—similarities and differences. *Curr. Opin. Colloid Interface Sci.* **2002**, *7* (1), 21–41.
- (3) Binks, B. P.; Horozov, T. S. *Colloidal Particles at Liquid Interfaces*; Cambridge University Press: Cambridge, 2006.
- (4) Boker, A.; He, J.; Emrick, T.; Russell, T. P. Self-assembly of nanoparticles at interfaces. *Soft Matter* **2007**, *3* (10), 1231–1248.
- (5) Pieranski, P. Two-dimensional interfacial colloidal crystals. *Phys. Rev. Lett.* **1980**, *45*, 569–572.
- (6) Hunter, T. N.; Pugh, R. J.; Franks, G. V.; Jameson, G. J. The role of particles in stabilising foams and emulsions. *Adv. Colloid Interface Sci.* **2008**, *137* (2), 57–81.
- (7) Dickinson, E. Food emulsions and foams: Stabilization by particles. *Curr. Opin. Colloid Interface Sci.* **2010**, *15* (1–2), 40–49.
- (8) Velev, O. D.; Furusawa, K.; Nagayama, K. Assembly of latex particles by using emulsion droplets as templates. 1. Microstructured hollow spheres. *Langmuir* **1996**, *12* (10), 2374–2384.
- (9) Dinsmore, A. D.; Hsu, M. F.; Nikolaides, M. G.; Marquez, M.; Bausch, A. R.; Weitz, D. A. Colloidosomes: Selectively permeable capsules composed of colloidal particles. *Science* **2002**, *298* (5595), 1006–1009.
- (10) Duan, H.; Wang, D.; Sobal, N. S.; Giersig, M.; Kurth, D. G.; Möhwald, H. Magnetic colloidosomes derived from nanoparticle interfacial self-assembly. *Nano Lett.* **2005**, *5* (5), 949–952.
- (11) Yow, H. N.; Routh, A. F. Release profiles of encapsulated actives from colloidosomes sintered for various durations. *Langmuir* **2009**, *25* (1), 159–166.
- (12) Cayre, O. J.; Hitchcock, J.; Manga, M. S.; Fincham, S.; Simoes, A.; Williams, R. A.; Biggs, S. pH-responsive colloidosomes and their use for controlling release. *Soft Matter* **2012**, *8* (17), 4717–4724.
- (13) Crossley, S.; Faria, J.; Shen, M.; Resasco, D. E. Solid nanoparticles that catalyze biofuel upgrade reactions at the water/oil interface. *Science* **2010**, *327* (5961), 68–72.
- (14) Wang, Z.; van Oers, M. C. M.; Rutjes, F. P. J. T.; van Hest, J. C. M. Polymersome colloidosomes for enzyme catalysis in a biphasic system. *Angew. Chem., Int. Ed.* **2012**, *51* (43), 10746–10750.
- (15) Vignati, E.; Piazza, R.; Lockhart, T. P. Pickering emulsions: Interfacial tension, colloidal layer morphology, and trapped-particle motion. *Langmuir* **2003**, *19* (17), 6650–6656.
- (16) Drelich, A.; Gomez, F.; Clausse, D.; Pezron, I. Evolution of water-in-oil emulsions stabilized with solid particles: Influence of added emulsifier. *Colloids Surf., A* **2010**, *365* (1–3), 171–177.
- (17) Levine, S.; Bowen, B. D.; Partridge, S. J. Stabilization of emulsions by fine particles II. capillary and van der Waals forces between particles. *Colloids Surf.* **1989**, *38* (2), 345–364.
- (18) Kutuzov, S.; He, J.; Tangirala, R.; Emrick, T.; Russell, T. P.; Boker, A. On the kinetics of nanoparticle self-assembly at liquid/liquid interfaces. *Phys. Chem. Chem. Phys.* **2007**, *9* (48), 6351–6358.
- (19) Kotula, A. P.; Anna, S. L. Probing timescales for colloidal particle adsorption using slug bubbles in rectangular microchannels. *Soft Matter* **2012**, *8* (41), 10759–10772.
- (20) Kim, J.; Cote, L. J.; Kim, F.; Yuan, W.; Shull, K. R.; Huang, J. Graphene oxide sheets at interfaces. *J. Am. Chem. Soc.* **2010**, *132* (23), 8180–8186.
- (21) Morse, A. J.; Tan, S.-Y.; Giakoumatos, E. C.; Webber, G. B.; Armes, S. P.; Ata, S.; Wanless, E. J. Arrested coalescence behaviour of giant Pickering droplets and colloidosomes stabilised by poly(tert-

butylaminoethyl methacrylate) latexes. *Soft Matter* **2014**, *10* (31), 5669–5681.

(22) Hunter, T. N.; Wanless, E. J.; Jameson, G. J.; Pugh, R. J. Non-ionic surfactant interactions with hydrophobic nanoparticles: Impact on foam stability. *Colloids Surf., A* **2009**, *347* (1–3), 81–89.

(23) Stocco, A.; Drenckhan, W.; Rio, E.; Langevin, D.; Binks, B. P. Particle-stabilised foams: an interfacial study. *Soft Matter* **2009**, *5* (11), 2215–2222.

(24) Du, K.; Glogowski, E.; Emrick, T.; Russell, T. P.; Dinsmore, A. D. Adsorption energy of nano- and microparticles at liquid–liquid interfaces. *Langmuir* **2010**, *26* (15), 12518–12522.

(25) Ferdous, S.; Ioannidis, M.; Henneke, D. Adsorption kinetics of alkanethiol-capped gold nanoparticles at the hexane–water interface. *J. Nanopart. Res.* **2011**, *13* (12), 6579–6589.

(26) Glaser, N.; Adams, D. J.; Böker, A.; Krausch, G. Janus particles at liquid–liquid interfaces. *Langmuir* **2006**, *22* (12), 5227–5229.

(27) Isa, L.; Amstad, E.; Schwenke, K.; Del Gado, E.; Ilg, P.; Kroger, M.; Reimhult, E. Adsorption of core-shell nanoparticles at liquid–liquid interfaces. *Soft Matter* **2011**, *7* (17), 7663–7675.

(28) Isa, L.; Calzolari, D. C. E.; Pontoni, D.; Gillich, T.; Nelson, A.; Zirbs, R.; Sanchez-Ferrer, A.; Mezzenga, R.; Reimhult, E. Core-shell nanoparticle monolayers at planar liquid–liquid interfaces: effects of polymer architecture on the interface microstructure. *Soft Matter* **2013**, *9* (14), 3789–3797.

(29) Alvarez, N. J.; Anna, S. L.; Saigal, T.; Tilton, R. D.; Walker, L. M. Interfacial dynamics and rheology of polymer-grafted nanoparticles at air–water and xylene–water interfaces. *Langmuir* **2012**, *28* (21), 8052–8063.

(30) Amalvy, J. I.; Unali, G. F.; Li, Y.; Granger-Bevan, S.; Armes, S. P.; Binks, B. P.; Rodrigues, J. A.; Whitby, C. P. Synthesis of sterically stabilized polystyrene latex particles using cationic block copolymers and macromonomers and their application as stimulus-responsive particulate emulsifiers for oil-in-water emulsions. *Langmuir* **2004**, *20* (11), 4345–4354.

(31) D'Souza Mathew, M.; Manga, M. S.; Hunter, T. N.; Cayre, O. J.; Biggs, S. Behavior of pH-sensitive core shell particles at the air–water interface. *Langmuir* **2012**, *28* (11), 5085–5092.

(32) Jaynes, E. N.; Flood, M. A. Protein films at oil–water interfaces: Interfacial tension measurements by the static drop method. *J. Dispersion Sci. Technol.* **1985**, *6* (1), 55–68.

(33) Li, G.; Prasad, S.; Dhinojwala, A. Dynamic interfacial tension at the oil/surfactant–water interface. *Langmuir* **2007**, *23* (20), 9929–9932.

(34) Binks, B. P.; Rodrigues, J. A. Types of phase inversion of silica particle stabilized emulsions containing triglyceride oil. *Langmuir* **2003**, *19* (12), 4905–4912.

(35) Binks, B. P.; Lumsdon, S. O. Pickering Emulsions Stabilized by Monodisperse Latex Particles: Effects of Particle Size. *Langmuir* **2001**, *17* (15), 4540–4547.

(36) Manga, M. S.; Cayre, O. J.; Williams, R. A.; Biggs, S.; York, D. W. Production of solid-stabilised emulsions through rotational membrane emulsification: influence of particle adsorption kinetics. *Soft Matter* **2012**, *8* (5), 1532–1538.

(37) Alvarez, N. J.; Walker, L. M.; Anna, S. L. Diffusion-limited adsorption to a spherical geometry: The impact of curvature and competitive time scales. *Phys. Rev. E: Stat., Nonlinear, Soft Matter Phys.* **2010**, *82* (1), 011604.

(38) Alvarez, N. J.; Walker, L. M.; Anna, S. L. A microtensiometer to probe the effect of radius of curvature on surfactant transport to a spherical interface. *Langmuir* **2010**, *26* (16), 13310–13319.

(39) Hansen, F. K. Surface dilatational elasticity of poly(oxyethylene)-based surfactants by oscillation and relaxation measurements of sessile bubbles. *Langmuir* **2008**, *24* (1), 189–197.

(40) Okubo, T. Surface Tension of Structured Colloidal Suspensions of Polystyrene and Silica Spheres at the Air–Water Interface. *J. Colloid Interface Sci.* **1995**, *171* (1), 55–62.

(41) Matsuoka, H.; Onishi, T.; Ghosh, A. pH-responsive non-surface-active/surface-active transition of weakly ionic amphiphilic diblock copolymers. *Colloid Polym. Sci.* **2014**, *292* (4), 797–806.

(42) Dan, A.; Gochev, G.; Miller, R. Tensiometry and dilatational rheology of mixed  $\beta$ -lactoglobulin/ionic surfactant adsorption layers at water/air and water/hexane interfaces. *J. Colloid Interface Sci.* **2015**, *449*, 383–391.

(43) Sharipova, A.; Aidarova, S.; Mucic, N.; Miller, R. Dilational rheology of polymer/surfactant mixtures at water/hexane interface. *Colloids Surf., A* **2011**, *391* (1–3), 130–134.

(44) Dan, A.; Wüstneck, R.; Krägel, J.; Aksenenko, E. V.; Fainerman, V. B.; Miller, R. Adsorption and dilatational rheology of mixed  $\beta$ -Casein/DoTAB layers formed by sequential and simultaneous adsorption at the water/hexane interface. *Langmuir* **2013**, *29* (7), 2233–2241.

(45) Freer, E. M.; Yim, K. S.; Fuller, G. G.; Radke, C. J. Interfacial rheology of globular and flexible proteins at the hexadecane/water interface: Comparison of shear and dilatation deformation. *J. Phys. Chem. B* **2004**, *108* (12), 3835–3844.

(46) Humblet-Hua, N.-P. K.; van der Linden, E.; Sagis, L. M. C. Surface rheological properties of liquid–liquid interfaces stabilized by protein fibrillar aggregates and protein–polysaccharide complexes. *Soft Matter* **2013**, *9* (7), 2154–2165.

(47) Yuan, Q.; Williams, R. A. CO-stabilisation mechanisms of nanoparticles and surfactants in Pickering Emulsions produced by membrane emulsification. *J. Membr. Sci.* **2016**, *497*, 221–228.